

Design and Testing of a Heaterless Hollow Cathode

Hakki Onur Dorduncu¹, Ishaan Mishra², Ben Mertz³

Rose-Hulman Institute of Technology, Terre-Haute, IN, 47803, United States of America

To promote undergraduate research on Hollow Cathodes, Rose-Hulman Electric Propulsion Group developed a low-current Heaterless Hollow Cathode. This paper presents the design and testing of a low-current Heaterless Hollow Cathode. Differences to conventional cathode designs, and a detailed testing procedure will be covered. Furthermore, a characterization setup will be proposed. Ignition of the cathode was achieved. However, a lack of discharge current was observed during the experimental campaign. The cathode was observed to be operating in space charge-limited mode.

I. Nomenclature

A	=	Vacuum breakdown equation constant
A_e	=	Emitter surface area
B	=	Vacuum breakdown equation constant
d_p	=	Emitter-orifice distance
d	=	Orifice diameter
EP	=	Electric Propulsion
γ_e	=	Fraction of the current due to secondary electrons
HC	=	Hollow Cathode
HHC	=	Heaterless Hollow Cathode
I_e	=	Current extracted
J	=	Electron current density
l	=	Orifice thickness
MFC	=	Mass Flow Controller
p	=	Pressure difference
P_1	=	Upstream pressure
P_2	=	Downstream pressure
Q	=	Flowrate
RHEPG	=	Rose-Hulman Electric Propulsion Group
T	=	Temperature
T_c	=	Critical temperature
T_R	=	Reduced temperature
V	=	Anode-cathode potential difference
V_b	=	Vacuum breakdown voltage
x	=	Anode-cathode distance
ζ	=	Viscosity

II. Introduction

Electrical Propulsion (EP) Systems use electrical power to increase the exhaust velocity of the propellant to achieve high specific impulse values in space missions [1]. EP thrusters like Gridded Ion Thrusters and Hall Thrusters utilize an essential subsystem called a Hollow Cathode (HC), which is a plasma source used to generate the discharge plasma and neutralize the plumes [2]. Heaterless Hollow Cathodes (HHCs) eliminate the requirement for a heater by using a

¹ Undergraduate Student, Department of Mechanical Engineering.

² Undergraduate Student, Department of Physics, Optical Engineering, and Nano Engineering.

³ Associate Professor of Mechanical Engineering, Department of Mechanical Engineering.

Paschen discharge to heat the insert to operating temperatures, reducing the number of required power supplies [2, 3, 4, 5]. HHCs ignite by a DC electrical breakdown of the propellant. The HHC has a grounded emitter, keeper, and anode in the circuit. With high pressure and potential difference in the keeper's orifice, the argon propellant can break down. The pressure difference between the sides of the orifice can be estimated using the Poiseuille equation [1]. The breakdown voltage required in the keeper's orifice can be estimated using the Paschen equation [6].

While many HHC studies can be found in literature they are not in flight-ready technical readiness level yet [7]. Most research is conducted in various graduate and professional labs, a limited number of undergraduate research teams have developed HHCs [8]. Work done by undergraduates can provide valuable experience for those at primarily undergraduate serving institutions seeking to get into the EP field. This paper presents the design and testing of a low-current HHC with an HCT-250-303-F Plasma Controls emitter [9]. The HHC was chosen to have a type C emitter orifice, which relies on heating by ion bombardment of the insert [1]. During the testing of the HHC Fixed Volume Release method, described in [10], was used to achieve ignition due to the limited flow rate provided by the Mass Flow Controllers (MFC) in the Rose-Hulman Electric Propulsion Group (RHEPG) laboratory. The HHC design consists of a keeper, chamber, backplate, and an emitter assembly. Additionally, an anode has been made as a part of the testing setup. The electrical circuitry for the HHC was also designed and constructed as a part of an internally-funded undergraduate research project at Rose-Hulman. A test setup including a thermocouple and a Langmuir probe was proposed. Design, testing, and proposed setup will be discussed in this paper to promote undergraduate research on HHCs.

III. Heaterless Hollow Cathode Ignition

A heater component is required for HCs to get ignition due to the need to reach thermionic temperatures for steady operation. Once the cathode reaches thermionic emission temperatures, ion bombardment and ion recombination processes due to the proximity of the plasma sustain the necessary emitter temperatures. The high-cycle thermal loading (along with design features such as geometry, material, insulation) can cause heaters to prematurely fail due to thermal fatigue [11]. Furthermore, heaters require significant power to operate. Getting rid of the heater could lead to reduced complexity and increased reliability of HC systems. HHCs use Paschen ignition, which is achieved under certain propellant pressures by the potential between the emitter material and insert material, to thermally prime the cathode system. The ignition is divided into three phases. The first phase is the electrical breakdown of the propellant. Electrical breakdown of the propellant causes plasma formation, heating the emitter material to thermionic emission temperatures. This is called the heating phase. Finally, the keeping phase is achieved at the thermionic emission temperatures and the cathode transitions into a steady state mode. [1,2,8]

IV. Development of The Heaterless Hollow Cathode & Anode

The HHC design was constrained by the complexity, cost, and availability of equipment in RHEPG. The complete exploded view of the HHC presented in Figure 1 has three regions: the keeper, the chamber, and the emitter assembly.

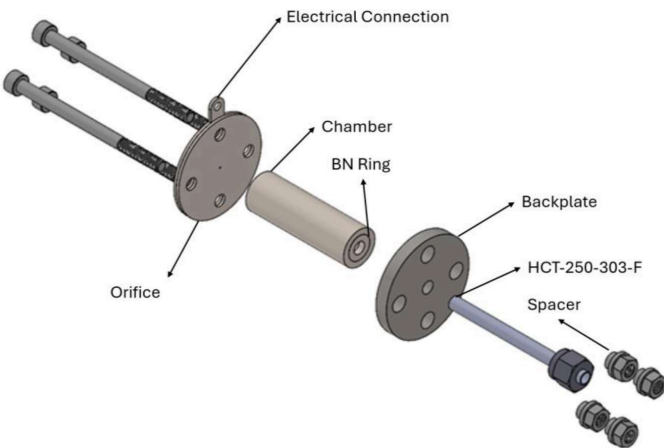


Figure 1: CAD design of the HHC. The HHC is split into three regions keeper, emitter, and chamber assembly.

The keeper was manufactured as two separate components (the orifice plate and an electrical connection) due to cost and manufacturing constraints. Considering the temperature range of the keeper described in [12], 1.51 mm (16-gauge) thickness steel was used as material for the orifice and electrical attachment. The orifice has an ID of 0.762 mm and a thickness of 1.4986 mm. The orifice, bolts, nuts, and electrical attachment were electrically isolated from the rest of the assembly using ceramic insulating spacers and the chamber. The chamber assembly consists of a ring and a chamber. The chamber was made from MACOR® ceramic and has an ID of 12.7 mm and a length of 59.182 mm. The chamber has a 3.175 mm hole for emitter temperature measurements using a thermocouple. The chamber was attached to the emitter assembly by a BN ring. The Plasma Controls HCT-250-303-F was chosen as the emitter assembly due to its affordability and availability. The assembly is held together by the backplate, which is made with low-carbon steel, considering the heat transfer models developed in [12].

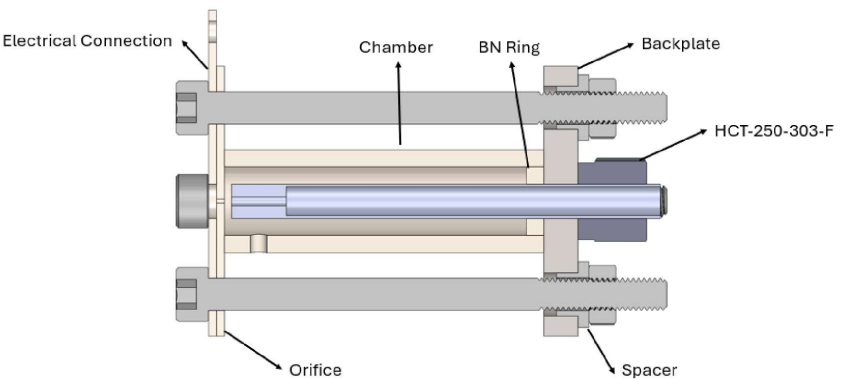


Figure 2: Cross-sectional view of the HHC.

An anode, shown in Figure 3, was required to make a complete circuit for testing purposes without the need of a thruster testbed. The anode was made out of spare materials at Rose-Hulman. The cylinder component in the anode was isolated from the rest of the assembly to be combined into the circuit. The rest of the anode consisted of a grounded mounting to the vacuum chamber. The assembly was connected by a ceramic bolt and nuts.

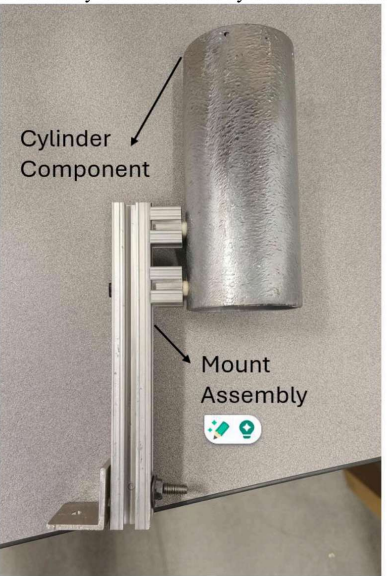


Figure 3: Anode assembly.

V.The Ignition Estimation Calculations of HHC

The HHC electrical setup consists of a Poweren P62B-4007.5 (400V 7.5A) for Ignition Power Supply (IPS), HP6632A (20V 5A) for Discharge Power Supply (DPS), STTH1210D (1000 V 12A) for diodes, and 100W 2Ω resistors as shown in Figure 4.

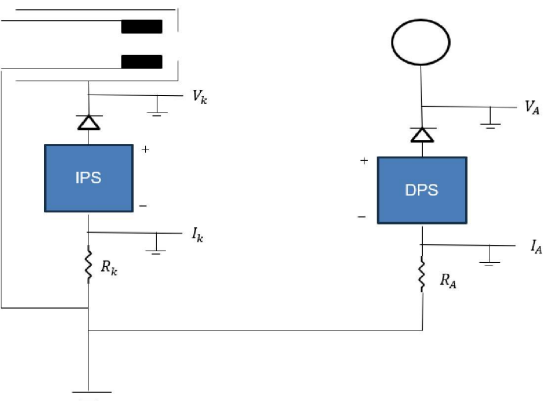


Figure 4: Electrical setup of the current HHC circuit.

To ignite the HHC, an electric breakdown of the argon propellant is needed. The viscosity of argon in poise is determined by following [13].

$$T_R = \frac{T}{T_C} \quad (1)$$

$$\zeta = 0.000167 T_R^{-618} - 0.000074 e^{-0.449 T_R} + 0.000071 e^{-4.058 T_R} + 3.736 \times 10^{-6} \quad (2)$$

The T_R and T_C represent the reduced and critical temperature of the propellant. The outputs ζ at $T = 293\text{K}$ are checked with [14], and 1% difference was observed. Then the flow equation for hollow cathodes in [1] was used to find the P_1 pressure upstream of the orifice in Torr

$$P_1 = \left(P_2^2 + 0.78 Q \zeta T_R \frac{l}{d^4} \right)^{\frac{1}{2}} \quad (3)$$

The $P_2 = 8 \times 10^{-6}$ Torr is the pressure of the downstream, $Q = 8 \text{ sccm}$ is the flowrate in sccm, l and d are thickness and diameter of the orifice. The voltage required to electrically breakdown propellant, V_b , was found by following [8]

$$V_b = B p \frac{d_p}{\ln(A p d_p) - \ln \left[\ln \left(1 + \frac{1}{\gamma_e} \right) \right]} \quad (4)$$

$p = 4.95$ Torr is the difference between the upstream and downstream of the orifice pressures. $A = 11.5 \frac{1}{\text{cm Torr}}$ and $B = 176 \frac{V}{\text{cm Torr}}$ are constant. d_p is the distance between the emitter and the orifice in cm. γ_e is the fraction of the current due to secondary electrons [14]. V_b is required to be 134.17V.

VI. The Test Procedure

The ignition was achieved by following the procedure described in [10]. The keeper voltage of 400V and current of 7.5A were applied. The system was pressurized in accordance with the Plasma Controls Manual [15]. The MFC was set at 8 sccm, and the valve between the cathode and MFC was shut. Once the valve was opened, the pressurized volume of propellant suddenly increased the mass flow rate, causing ignition to be achieved as shown in Figure 5.



Figure 5: Picture of HHC design during ignition tests.

VII. Proposed Characterization Setup

A testing procedure for characterization of the HHC was designed and assembled, however data was not able to be collected in time to be included in this paper. The proposed setup is described in this section to show what is needed to characterize the system performance. A thermocouple and a Langmuir probe were set up in the vacuum chamber to measure the emitter temperature and relate that to properties of the plasma plume. The Langmuir probe was mounted inside the anode to align with the center of the cathode. A Keysight DSO7014B oscilloscope was sourced to measure emitter-keeper voltage & current, and Langmuir probe measurements. The experimental setup is shown in Figure 6, where the thermocouple is located on the left side, going through the chamber and attached to the emitter assembly. The anode is located at the top side of the picture, housing the Langmuir probe.

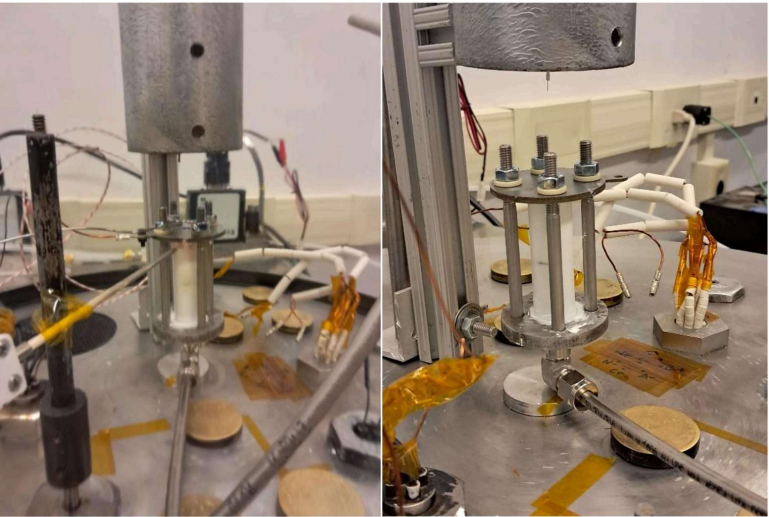


Figure 6: Experimental setup inside the vacuum chamber.

An Evolution Sensors 152.4 mm long, 3.175 mm diameter, ungrounded Type C Thermocouple was selected to measure the emitter temperature to help validate a 1D heat model, which helps us understand the thermionic current of the emitter material [1]. I-V characteristics obtained by the Langmuir probe would allow us to determine plasma properties such as electron temperature and plasma density [16]. The keeper-emitter current and voltage would be used to understand cathode ignition phases, such as breakdown, heating, and keeping [2, 17, 18].

VIII. Results

After ignition, the keeper voltage converged to 12V, and discharge was observed. Spot mode and Plume mode are the two typical types of HHC discharges [1]. Discharge was observed to be in spot mode, as shown in Figure 7.



Figure 7: Heaterless Hollow Cathode discharge at 8 sccm.

However, neither discharge current nor readings from the Langmuir probe were observed, which is not fully understood. A possible explanation is a low current between the cathode and the anode due to space-charge limited

current flow. The electron extraction from cathodes is limited by temperature-limited mode and space charge-limited mode. Temperature-limited mode is governed by the Richardson-Dushman equation, which defines the relationship between the emitted current density and the temperature of the emitter material. Space charge limited mode is governed by Child-Langmuir equation described in [1].

$$J = 2.33 \times 10^{-6} \frac{V^2}{x^2} \quad (5)$$

V is the potential difference between the anode and cathode. x is the distance between the cathode and the anode. The expected current extracted can be calculated by

$$I_e = JA_e \quad (6)$$

A_e is the surface area of the emitter. Because the potential difference is low, and the anode-cathode distance is high, the extracted current cannot be observed. The maximum available voltage of 20V for the anode makes the potential difference 8V over the 7.5 cm gap, causing the extracted current to be expected at 5×10^{-7} A, so low that it cannot be observed. Unfortunately, the RHEPG did not have functional power supplies that had a higher maximum voltage to replace the DPS. The anode could not be replaced due to the time constraints.

IX. Conclusion

The design and testing of an all undergraduate-designed/built Heaterless Hollow Cathode was presented in this paper. The Mini Plasma Lab described in [19] was used to test the HHC, which resulted in a visible plasma discharge. The Fixed Volume Release method was used to achieve ignition. The lack of discharge current was observed due to the space-limited mode charge. For future testing, power supplies with greater voltage limits can be used, or the anode dimension can be modified. The HHC presented can be treated as an initial prototype, with successful ignition. However, future improvements have to be made in the anode setup for the characterization of HHC.

Acknowledgments

This project was funded by the Rose-Hulman Independent Project/Research Opportunities Program, the Noblitt Scholars Program, the Student Government Association, and an internal college student research grant. The authors thank Hao Yejia for his support with the electrical schematic and component selection, Roger Sladek for manufacturing parts, Brian Fair for assisting with vacuum chamber operation, and Dr. Marc Herniter for lending a power supply. We would also like to thank Casey Farnell and Cody Farnell for their assistance with the emitter material. ChatGPT is used to crop tools, such as a caliper, in the Figure 3 for making it clearer to the audience.

References

- [1] D. M. Goebel and I. Katz, Fundamentals of Electric Propulsion: Ion and Hall Thrusters 2nd Edition, Hoboken, NJ: Wiley, 2023.
- [2] V. Vekselman, Y. E. Krasik, S. Gleizer, V. T. Gurovich, A. Warshavsky and L. Rabinovich, "Characterization of a Heaterless Hollow Cathode," AIAA Propulsion and Power, vol. 29:2, no. 2, pp. 475-486, 2013.
- [3] W. -C. Wang, Y. -L. Huang, J. H. Hsieh, J. Heri and Y. -H. Li, "Development of heaterless hollow cathode for low-power Hall thruster," in IEEE International Conference on Aerospace Electronics and Remote Sensing Technology (ICARES), Bali, Indonesia, 2023.
- [4] A. R. Payman and D. M. Goebel, "Development of a 50-A heaterless hollow cathode for electric thrusters," Jet Propulsion Laboratory, California Institute of Technology, Pasadena, California 91109, USA, 2022.
- [5] M. Schatz, "Heaterless ignition of inert gas ion thruster hollow cathodes," in International Electric Propulsion Conference, Alexandria, VA, U.S.A., 1985.
- [6] M. A. L. a. A. J. Lichtenberg, Principles of Plasma Discharges and Materials Processing, Hoboken, New Jersey: John Wiley & Sons Inc., 2005.
- [7] A. Nikrant, "Development and Modelling of a Low Current LaB6," Virginia Polytechnic Institute and State University, Blacksburg, 2019.

- [8] J. Wetherbee, D. Torres, S. Hering, S. Padilla, G. Gustavson, K. Korte-Wormley, O. Mokatish, S. Mhaske, N. Cruz, G. Ostrander and H. V. Nguyen, "Student Design and Analysis of a Hall Effect Thruster," in AIAA Scitech Forum, National Harbor, MD & Online, 2023.
- [9] C. Farnell, C. Farnell, J. Williams, D. Williams, B. G. Nguyen, K. E. Greiner and R. K. Ham, "Simplified Formation Process of a Low Work Function Insert". CO, USA Patent US10002738B1, 19 June 2018.
- [10] R. K. Ham, J. D. Williams and S. J. Thompson, "A Low Erosion Instant Start Ignition Process for Heaterless Hollow Cathodes," in AIAA Propulsion and Energy Forum, 2021.
- [11] R. K. Ham, "An Experimental Investigation of Heaterless Hollow Cathode Ignition," Colorado State University, Fort Collins, Colorado, 2020.
- [12] U. Kokal, N. Turan and M. Celik, "Thermal Analysis and Testing of Different Designs of LaB6 Hollow Cathodes to Be Used in Electric Propulsion Applications," Aerospace, vol. 8, no. 8, 2021.
- [13] R. C. Reid, The Properties of Gases, New York : McGrawHill, 1977.
- [14] M. Daksha, B. Berger, E. Schuengel, I. Korolov, A. Derzsi, M. Koepke, Z. Donkó and J. Schulze, "A computationally assisted spectroscopic technique to measure secondary electron emission coefficients in radio frequency plasmas." Journal of Physics D: Applied Physics, vol. 49, no. 23, 2016.
- [15] "201-0140 Cathode Assembly," Plasma Controls, 2024.
- [16] R. B. Lobbia and B. E. Beal, "Recommended Practice for Use of Langmuir Probes in Electric Propulsion Testing," Journal of Propulsion and Power, vol. 33, no. 3, 2017.
- [17] A. Nikrant, P. Jain and C. Adams, "Experimental Characterization of Gas Pressure and Flow Rate Across Heaterless Hollow Cathode Orifices," Journal of Propulsion and Power, vol. 37, no. 5, pp. 801-805, 2021.
- [18] D. R. Lev, I. G. Mikellides, D. Pedrini, D. M. Goebel, B. A. Jorns and M. S. McDonald, "Recent progress in research and development of hollow cathodes for electric propulsion," Reviews of Modern Plasma Physics, vol. 3, no. 1, pp. 3-12, 2019.
- [19] I. Mishra, T. Ausec, H. O. Dorduncu, A. Jirovec, J. Lin and M. Vasquez, "Development of an Undergraduate DC-Discharge Ring-Cusp Miniature Gridded Ion Thruster," in IEEE Aerospace Conference, Big Sky, MT, USA, 2024.